

HistDiST: Histopathological Diffusion-based Stain Transfer

Erik Großkopf*, Valay Bundele*, Mehran Hossienzadeh*,
Hendrik P.A. Lensch

University of Tübingen, Germany
erik.grosskopf@student.uni-tuebingen.de, {valay.bundele,
mehr.hosseinzadeh, hendrik.lensch}@uni-tuebingen.de

Abstract. Hematoxylin and Eosin (H&E) staining is the cornerstone of histopathology but lacks molecular specificity. While Immunohistochemistry (IHC) provides molecular insights, it is costly and complex, motivating H&E-to-IHC translation as a cost-effective alternative. Existing translation methods are mainly GAN-based, often struggling with training instability and limited structural fidelity, while diffusion-based approaches remain underexplored. We propose HistDiST, a Latent Diffusion Model (LDM) based framework for high-fidelity H&E-to-IHC translation. HistDiST introduces a dual-conditioning strategy, utilizing Phikon-extracted morphological embeddings alongside VAE-encoded H&E representations to ensure pathology-relevant context and structural consistency. To overcome brightness biases, we incorporate a rescaled noise schedule, v -prediction, and trailing timesteps, enforcing a zero-SNR condition at the final timestep. During inference, DDIM inversion preserves the morphological structure, while an η -cosine noise schedule introduces controlled stochasticity, balancing structural consistency and molecular fidelity. Moreover, we propose Molecular Retrieval Accuracy (MRA), a novel pathology-aware metric leveraging GigaPath embeddings to assess molecular relevance. Extensive evaluations on MIST and BCI datasets demonstrate that HistDiST significantly outperforms existing methods, achieving a 28% improvement in MRA on the H&E-to-Ki67 translation task, highlighting its effectiveness in capturing true IHC semantics.

Keywords: Stain Transfer · Diffusion Models · Digital Pathology

1 Introduction

Histopathology is essential for disease diagnosis, revealing tissue structure and cellular morphology. While Hematoxylin and Eosin (H&E) staining is cost-effective and highlights structural details, it lacks molecular specificity. In contrast, Immunohistochemistry (IHC) provides molecular insights but is expensive and time-consuming. Automated H&E-to-IHC translation offers a scalable solution by inferring molecular details from tissue morphology, reducing costs, and

* These authors contributed equally to the work.

enhancing diagnostic consistency. GANs have shown promise in this task. Li et al. [2] use adaptive supervised PatchNCE loss to preserve structure, while MDCL [10] employs a conditional GAN with multi-domain contrastive learning to enhance cross-domain alignment. Pathology-specific approaches include patch-level feature extraction with multiple instance learning [4] and HER2 scoring enhancement via nuclei density estimation [9]. However, GANs still face mode collapse and require complex loss designs to maintain consistency in pathology screenings.

Recently, diffusion models (DMs) [18] have emerged as a powerful alternative, offering superior stability and synthesis quality. Latent Diffusion Models (LDMs) [19] reduce the computational burden of DMs by operating in the latent space of pretrained autoencoders. LDM-based image editing methods, such as Instruct-Pix2Pix [21] for instruction-based editing and ControlNet [8] for conditional generation, offer structured control. Inference-time optimization techniques using DDIM Inversion [23] and Delta Denoising Score [24] further enhance structural fidelity. Although there has been quite some work on applying LDMs for natural image editing, the application of LDMs for H&E-to-IHC stain translation remains largely unexplored. Existing diffusion-based methods [12][13] mainly use text prompts or unpaired signal vector conditioning, but often fail to ensure structural and semantic consistency, critical for accurate pathology translation.

To address these limitations, we propose HistDiST, an LDM-based framework for high-fidelity H&E-to-IHC stain translation. Although LDM offers strong generative capabilities, its direct application to stain translation faces three key challenges: (i) lack of explicit morphological conditioning, (ii) brightness bias from conventional diffusion noise schedules, and (iii) insufficient structural preservation at inference. These limitations hinder the model’s ability to capture complex morphology–molecular relationships and lead to inaccurate brightness distributions that obscure diagnostically relevant molecular features.

HistDiST overcomes these challenges through three key contributions. First, a dual-conditioning strategy integrates Phikon-based [20] pathology-specific embeddings into the U-Net’s cross-attention layers and concatenates VAE-encoded H&E representations with the input latent noise. This ensures that pathology-relevant context guides denoising for precise molecular reconstruction. Second, to address brightness inconsistencies, we incorporate a rescaled noise schedule and trailing timesteps [26] along with v -prediction [25], enforcing zero terminal SNR. Third, we perform joint training for unconditional H&E generation and H&E-to-IHC translation, a critical step that enables the use of DDIM inversion [16] for structure preservation at inference. However, the deterministic nature of DDIM sampling restricts generative flexibility, limiting the model’s ability to capture subtle molecular variations critical for accurate IHC synthesis. To mitigate this, we incorporate an η -cosine noise schedule, progressively increasing the noise scale during denoising to enable stochastic exploration. This significantly improves FID scores while preserving both morphological structures and molecular fidelity in the translated IHC images. Moreover, we propose a novel feature-based metric, Molecular Retrieval Accuracy (MRA), that assesses molecular fidelity via cosine similarity. Experiments on the MIST and BCI datasets

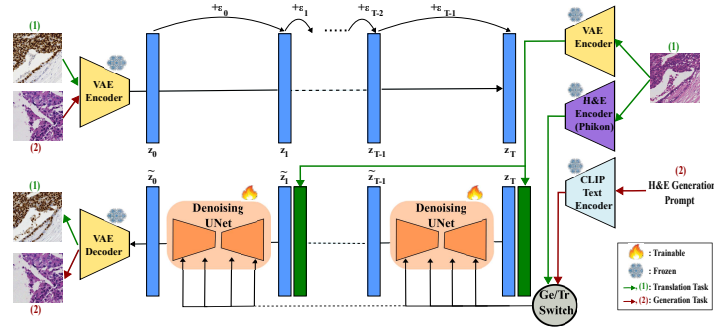


Fig. 1. HistDiST training pipeline, showing H&E generation (red arrows, label (2)) conditioned on CLIP text embeddings, and H&E-to-IHC translation (green arrows, label (1)) guided by Phikon embeddings and VAE-encoded H&E features. The VAE encoder maps images to latent space, where noise is added and later denoised by the U-Net. The Ge/Tr switch selects between generation and translation tasks, with each (numbered input, color-coded pathway) independently followed.

demonstrate that HistDiST outperforms state-of-the-art methods across both qualitative and quantitative metrics, achieving superior visual fidelity, structural preservation, and molecular fidelity. Notably, HistDiST shows 28% improvement on MRA on H&E-to-Ki67, demonstrating highly accurate IHC synthesis.

2 Methodology

2.1 Preliminaries

Diffusion models generate data by learning to reverse a stochastic forward process that gradually corrupts an input sample x_0 with Gaussian noise over T steps, following a variance schedule β_t : $q(x_t|x_{t-1}) = \mathcal{N}(x_t; \sqrt{1-\beta_t}x_{t-1}, \beta_t I)$. For large T , this process converges to an isotropic Gaussian distribution. The model approximates the reverse process, $p_\theta(x_{t-1}|x_t) = \mathcal{N}(x_{t-1}; \mu_\theta(x_t, t), \Sigma_\theta(x_t, t))$ where μ_θ and Σ_θ are learnable functions. Training involves predicting the noise component $\epsilon_\theta(x_t, t)$ by minimizing: $L = \mathbb{E}_{x_0, t, \epsilon} [\|\epsilon - \epsilon_\theta(x_t, t)\|^2]$, where $\epsilon \sim \mathcal{N}(0, I)$ and ϵ_θ is a neural network parameterized by θ . Latent Diffusion Models (LDMs) enhance computational efficiency by operating in a compressed latent space, where an encoder E maps images x_0 to latent representations $z_0 = E(x_0)$.

2.2 HistDiST

We present HistDiST, a novel framework leveraging LDM for high-fidelity H&E-to-IHC stain translation. LDM operate in a variational autoencoder (VAE) latent space and use a U-Net denoising network with residual connections, self-attention, and cross-attention mechanisms. HistDiST achieves superior structural and molecular accuracy through: (1) dual-conditioning (2) v-prediction

with rescaled noise schedules, and (3) DDIM inversion with η -cosine scheduling balancing determinism with controlled stochasticity.

Dual Conditioning: To capture the intricate relationship between tissue morphology and molecular expression, HistDiST employs a *dual-conditioning* strategy. First, Phikon [20], a self-supervised transformer trained on 40 million histology images, extracts morphological feature embeddings from the input H&E-stained image. These embeddings are injected into the cross-attention layers of the U-Net, enabling the model to integrate pathology-relevant context throughout the denoising process. Second, inspired by InstructPix2Pix [21], we modify the U-Net by applying additional input channels that allow VAE-encoded H&E latents to be concatenated with the latent noise vector at the U-Net input. This modification provides structural guidance from the earliest denoising stages, enabling IHC generation with high structural fidelity and molecular accuracy.

Joint Training: Fig. 1 shows the training pipeline of HistDiST. To enable DDIM inversion for structure preservation at inference, HistDiST is trained jointly on unconditional H&E generation and H&E-to-IHC translation. While the VAE remains frozen, the U-Net is fine-tuned on paired H&E-IHC data. A key limitation in standard diffusion models is that common noise schedules fail to enforce zero SNR at the final timestep, causing residual low-frequency information to be leaked during training [26]. However, at inference, the model starts from pure Gaussian noise, leading to a mismatch between training and inference, resulting in constrained brightness levels. HistDiST addresses this by rescaling the noise schedule under a variance-preserving formulation [26] to enforce zero terminal SNR and enable more accurate brightness distribution in outputs.

Moreover, when SNR is zero, traditional epsilon (ϵ) prediction becomes trivial and does not provide meaningful learning signals. To overcome this, HistDiST adopts a v -prediction and v -loss framework as proposed in [25]. The velocity vector is defined as $v_t = \sqrt{\bar{\alpha}_t} \epsilon - \sqrt{1 - \bar{\alpha}_t} x_0$, where x_0 is the clean latent representation (noise-free image), ϵ is the Gaussian noise added during the forward diffusion process, and $\bar{\alpha}_t$ represents the cumulative product of the noise schedule parameters up to timestep t . The corresponding v -prediction loss function is:

$$\mathcal{L} = \lambda_t \|v_t - \tilde{v}_t\|_2^2 \tag{1}$$

where v_t is the true velocity, \tilde{v}_t is the velocity predicted by the network, and λ_t is a timestep-dependent weighting factor. Finally, HistDiST employs trailing timestep selection, prioritizing later timesteps during training to align with inference, where model starts from pure Gaussian noise. This enables generation of images with diverse brightness levels and helps preserve molecular features.

Inference: Fig. 2 (Left) shows the inference pipeline. Preserving the *morphological structure* of input images is essential for H&E-to-IHC stain translation. To achieve this, we employ DDIM inversion [16] to map input H&E representation z_0 to its corresponding noise vector z_T . This inversion process effectively "reverses" the generative path, allowing us to find the specific noise that encodes

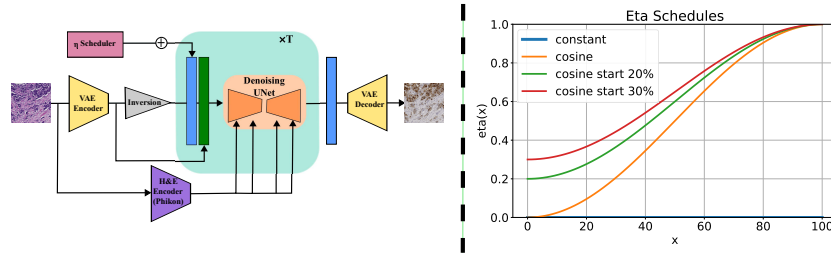


Fig. 2. HistDiST inference pipeline (Left): VAE encoder maps H&E image to latent space, where DDIM inversion derives noise and η -noise scheduling injects noise at different timesteps during denoising. The U-Net, conditioned on Phikon embeddings, refines the features, and the VAE decoder generates the final IHC output. (Right) η -schedules, with cosine-start schedules optimizing FID and structural preservation.

structural elements of the input. By using the inverted noise z_T and then sampling with the trained HistDiST, we obtain translated images that maintain the original morphological features while rendering them in the target IHC modality.

The inversion is performed via deterministic updates:

$$z_{t+1} = \sqrt{\alpha_{t+1}} \left(\frac{z_t - \sqrt{1 - \alpha_t} \epsilon_\theta(z_t, t, c_T)}{\sqrt{\alpha_t}} \right) + \sqrt{1 - \alpha_{t+1}} \epsilon_\theta(z_t, t, c_T) \quad (2)$$

where α_t is the cumulative noise schedule, ϵ_θ is the predicted noise, and c_T is the text-based conditioning embedding. While using this inverted noise as the starting point for translation successfully preserved structural features, we observed an increase in FID scores (Table 2 (right), $\eta=0$), indicating that deterministic DDIM sampling restricted generative flexibility and hindered the model’s ability to capture molecular diversity essential for accurate IHC synthesis.

To address this, we incorporated an η -cosine noise schedule that introduces *controlled stochasticity* during denoising. Unlike standard deterministic DDIM sampling, our schedule progressively increases the noise scale η_t from a non-zero initial value following a cosine schedule:

$$\eta_t(t) = 0.6 - 0.4 \cos \left(\pi \frac{t}{T} \right)$$

where T is the total number of diffusion steps, and t is the current timestep. The denoising update then becomes:

$$z_{t-1} = \sqrt{\alpha_{t-1}} \left(\frac{z_t - \sqrt{1 - \alpha_t} \epsilon_\theta(z_t, t)}{\sqrt{\alpha_t}} \right) + \sqrt{1 - \alpha_{t-1} - \sigma_t^2} \cdot \epsilon_\theta(z_t, t) + \sigma_t \cdot \eta_t \cdot \epsilon \quad (3)$$

where σ_t is diffusion step-size parameter and $\epsilon \sim \mathcal{N}(0, I)$. By progressively increasing η_t from 0.2 to 1.0, the schedule fosters stochastic exploration during translation while maintaining structural coherence. The integration of η -cosine noise schedule lowered FID scores (Table 2 (right), η cosine start 20%), effectively striking a balance between morphological preservation and molecular fidelity.

Table 1. Evaluations on all translation tasks in the datasets, showing our superlative performance in almost all metrics. For PHV, $T = 0.01$ and KIDs are multiplied by 1K.

Dataset	Method	SSIM \uparrow	PHV $_{L1}$ \downarrow	PHV $_{L2}$ \downarrow	PHV $_{L3}$ \downarrow	PHV $_{L4}$ \downarrow	MRA \uparrow	FID \downarrow	KID \downarrow
MIST $_{ER}$	CycleGAN	0.1982	0.5175	0.5092	0.3710	0.8672	0.235	125.7	95.1
	Pix2Pix	0.1500	0.5818	0.5282	0.3700	0.8620	-	128.1	79
	PyramidP2P	0.2172	0.4767	0.4538	0.3757	0.8567	-	107.4	84.2
	ASP	0.2061	0.4336	0.4007	0.2649	0.8205	0.248	41.4	5.8
	MDCL	0.2005	0.4533	0.3969	0.2646	0.8238	0.322	34.9	3.6
	HistDiST	0.2278	0.3645	0.3105	0.2465	0.8226	0.552	31.2	3.6
MIST $_{HER2}$	ASP	0.2004	0.4534	0.4150	0.2665	0.8174	0.193	51.4	12.4
	MDCL	0.1810	0.4371	0.3944	0.2518	0.8171	0.233	44.4	7.5
	HistDiST	0.2059	0.3830	0.3298	0.2512	0.8245	0.466	36.9	3.8
MIST $_{Ki67}$	ASP	0.2410	0.4472	0.4001	0.2701	0.8128	0.148	51	19.1
	MDCL	0.2236	0.4005	0.3638	0.2465	0.8064	0.201	30.8	6.1
	HistDiST	0.2463	0.3375	0.2893	0.2311	0.8174	0.484	28.05	4.4
MIST $_{PR}$	ASP	0.2159	0.4484	0.3898	0.2564	0.8080	0.237	44.8	10.2
	MDCL	0.2081	0.4320	0.3768	0.2499	0.8052	0.317	38.3	7.1
	HistDiST	0.2381	0.4001	0.3355	0.2598	0.8265	0.434	33.7	4.3
BCI $_{HER2}$	ASP	0.5032	0.4308	0.3670	0.2235	0.7210	0.058	65.1	9.9
	MDCL	0.5029	0.4962	0.3861	0.2351	0.7344	0.084	51.2	13
	HistDiST	0.4693	0.3136	0.2943	0.2165	0.7063	0.218	34.2	5.6

3 Experiments

Datasets: We evaluate on two public H&E-to-IHC datasets: (1) MIST [2]: Paired H&E patches (1024×1024) with four IHC stains—HER2, Ki67, ER, and PR—using around 4k training pairs per stain and 1000 test pairs each. (2) BCI [7]: H&E–HER2 pairs (1024×1024) with 3896 training and 977 test samples.

Implementation Details: We fine-tune Stable Diffusion v1.5, training for 500 epochs with a batch size of 16. AdamW optimization is used with a $2e - 4$ learning rate, 1000 warmup steps, and a cosine decay schedule. Training alternates between H&E generation and H&E-to-IHC translation. v -prediction is set to $\gamma = 5$, and noise schedule is rescaled to enforce zero terminal SNR.

Evaluation Metrics: We use both unpaired and paired metrics to assess image quality and molecular fidelity. Unpaired metrics include FID and KID for distributional similarity. Paired metrics include SSIM for image quality and PHV [14] for feature-level relevance. To capture pathology-specific semantics, we introduce Molecular Retrieval Accuracy (MRA), a novel metric leveraging GigaPath [15], a pathology foundation model trained on H&E and IHC data. MRA measures molecular fidelity by determining whether predicted IHC embedding best matches its ground-truth counterpart among all IHC embeddings in the test set using cosine similarity.

Table 2. Ablation study (on ER) during training (left) and inference (right). Abbreviations: "SD+IC": Stable Diffusion with input conditioning based on VAE-extracted H&E features, " v -pred": v -prediction, "Inv": DDIM Inversion with η -cosine start 20% noise (for DDIM sampling), "xAtt": cross-attention with Phikon-extracted H&E features. The inference strategies involve DDIM inversion for structure preservation, followed by DDIM sampling with different noise schedules (illustrated in Fig. 2 (right))

Training Strategy	SSIM \uparrow	PHV $_{avg}$ \downarrow	FID \downarrow	Inference Strategy	PHV $_{avg}$ \downarrow	MRA \uparrow	FID \downarrow
SD+IC	0.116	0.599	106.5	η constant	0.4500	0.598	41.7
SD+IC, v p	0.198	0.501	37.5	η cosine	0.4426	0.559	34.3
SD+IC, v p, Inv	0.228	0.511	41.3	η cosine start 20%	0.4360	0.552	31.3
SD+IC, v p, Inv, xAtt	0.227	0.436	31.3	η cosine start 30%	0.4328	0.547	30.1

Results: We compare HistDiST with state-of-the-art stain translation models—CycleGAN [5], Pix2Pix [6], PyramidP2P [7], ASP [2], and MDCL [10]—for H&E-to-ER translation. For other transfer tasks, we select the top two performers for comparison. As shown in Table 1, HistDiST achieves consistent performance gains across all key metrics. It achieves the highest MRA scores, surpassing MDCL by 23% on MIST_{ER} and MIST_{HER2}, demonstrating superior molecular fidelity. It also attains the lowest PHV scores, indicating better feature-space alignment, and the best FID/KID scores, confirming that the generated IHC images are more visually realistic and distributionally aligned with real ones.

Ablation Studies: Table 2 (Left) and Fig. 3 present the quantitative and qualitative impact of different components in our framework. Fine-tuning Stable Diffusion with input conditioning alone on the paired dataset results in poor structural preservation and low molecular fidelity, leading to significant performance degradation across all metrics. Integrating v -prediction improves molecular expression patterns, enhancing FID scores and feature-space alignment. However, structural inconsistencies persist (as can also be seen in Fig. 3), indicating that direct adaptation remains insufficient for accurate stain translation. To address this, we conduct joint training on H&E generation and H&E-to-IHC translation, and at inference apply DDIM inversion followed by DDIM sampling with η cosine start 20% noise schedule, which greatly enhances structural preservation. Finally, incorporating Phikon-extracted morphological embeddings into U-Net’s cross-attention layers further refines feature-space alignment and enhances structural integrity and molecular fidelity, yielding the best overall performance. This demonstrates that explicit pathology-aware conditioning is critical for accurate molecular reconstruction and high-fidelity stain translation. In most of the cases, MDCL often introduces artifacts or fails to capture fine molecular details, whereas HistDiST better preserves molecular expression patterns and produces more precise IHC intensity distributions, aligning closely with GT IHC.

Table 2 (right) and Fig. 4 examine the effect of different η -noise schedules at inference, with Fig. 2 (right) visualizing the tested schedules. Setting $\eta = 0$ yields optimal structural alignment between input H&E and translated IHC but

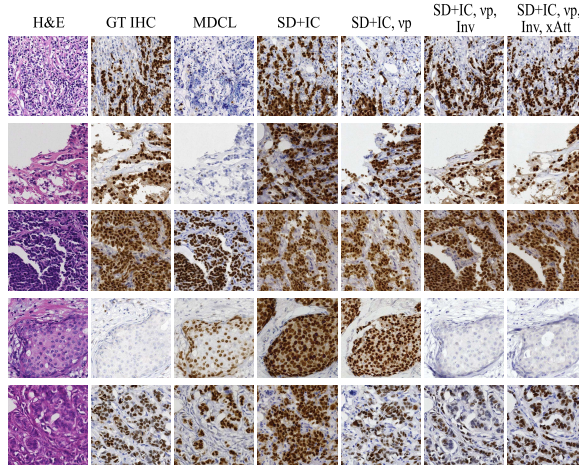


Fig. 3. ER translation outputs across methods (see Table 2 for abbreviations).

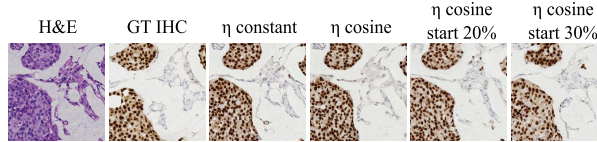


Fig. 4. ER translation outputs across noise schedules (see Table 2 for abbreviations).

results in high FID scores, indicating a poor match to the real IHC distribution. Introducing a cosine noise schedule starting from zero improves FID scores while preserving structural integrity, suggesting that injecting controlled stochasticity at higher timesteps promotes distributional alignment with real IHC data. Increasing the starting noise level to 0.2 further reduces FID scores with minimal structural loss, while increasing it to 0.3 introduces noticeable structural deviations, despite additional improvements in FID. To balance structural preservation, molecular fidelity, and distributional realism, we adopt the cosine schedule starting at 0.2 as the optimal configuration.

4 Conclusion

We present HistDiST, an LDM-based framework for H&E-to-IHC stain translation, integrating pathology-aware conditioning, DDIM inversion, and zero terminal SNR enforcement to enhance structural fidelity and molecular accuracy. We also introduce Molecular Retrieval Accuracy (MRA), a novel metric for pathology-aware evaluation. Experiments on MIST and BCI datasets demonstrate that HistDiST achieves superior visual fidelity, molecular accuracy and structural preservation compared to the existing approaches.

5 Acknowledgments

The work described in this paper was conducted in the framework of the Graduate School 2543/1 "Intraoperative Multi-Sensory Tissue Differentiation in Oncology" (project ID 40947457) funded by the German Research Foundation (DFG - Deutsche Forschungsgemeinschaft). This work has been supported by the Deutsche Forschungsgemeinschaft (DFG) – EXC number 2064/1 – Project number 390727645. The authors thank the International Max Planck Research School for Intelligent Systems (IMPRS-IS) for supporting Valay Bundele and Mehran Hosseinzadeh.

References

1. Salimans, Tim and Ho, Jonathan: Progressive distillation for fast sampling of diffusion models. In: arXiv preprint arXiv:2202.00512. (2022)
2. Li, Fangda, Hu, Zhiqiang, Chen, Wen, Kak, Avinash: Adaptive supervised patchnce loss for learning H&E-to-IHC stain translation with inconsistent groundtruth image pairs. In: Proceedings of the International Conference on Medical Image Computing and Computer-Assisted Intervention. pp. 632–641 (2023)
3. Chen, Fuqiang, Zhang, Ranran, Zheng, Boyun, Sun, Yiwen, He, Jiahui, Qin, Wenjian: Pathological semantics-preserving learning for H&E-to-IHC virtual staining. In: Proceedings of the International Conference on Medical Image Computing and Computer-Assisted Intervention. pp. 384–394 (2024)
4. Li, Jiahao, Dong, Jiuyang, Huang, Shenjin, Li, Xi, Jiang, Junjun, Fan, Xiaopeng, Zhang, Yongbing: Virtual Immunohistochemistry Staining for Histological Images Assisted by Weakly-supervised Learning. In: Proceedings of the IEEE/CVF Conference on Computer Vision and Pattern Recognition. pp. 11259–11268 (2024)
5. Zhu, Jun-Yan and Park, Taesung and Isola, Phillip and Efros, Alexei A: Unpaired image-to-image translation using cycle-consistent adversarial networks. In: Proceedings of the IEEE international conference on computer vision. pp. 2223–2232 (2017)
6. Isola, Phillip and Zhu, Jun-Yan and Zhou, Tinghui and Efros, Alexei A: Image-to-image translation with conditional adversarial networks. In: Proceedings of the IEEE conference on computer vision and pattern recognition. pp. 1125–1134 (2017)
7. Liu, Shengjie and Zhu, Chuang and Xu, Feng and Jia, Xinyu and Shi, Zhongyue and Jin, Mulan: Bci: Breast cancer immunohistochemical image generation through pyramid pix2pix. In: Proceedings of the IEEE/CVF conference on computer vision and pattern recognition. pp. 1815–1824 (2022)
8. Zhang, Lvmin and Rao, Anyi and Agrawala, Maneesh: Adding conditional control to text-to-image diffusion models. In: Proceedings of the IEEE/CVF international conference on computer vision. pp. 3836–3847 (2023)
9. Peng, Qiong, Lin, Weiping, Hu, Yihuang, Bao, Ailisi, Lian, Chenyu, Wei, Weiwei, Yue, Meng, Liu, Jingxin, Yu, Lequan, Wang, Liansheng: Advancing H&E-to-IHC Virtual Staining with Task-Specific Domain Knowledge for HER2 Scoring. In: Proceedings of the International Conference on Medical Image Computing and Computer-Assisted Intervention. pp. 3–13 (2024)
10. Wang, Song, Zhang, Zhong, Yan, Huan, Xu, Ming, Wang, Guanghui: Mix-Domain Contrastive Learning for Unpaired H&E-to-IHC Stain Translation. arXiv preprint arXiv:2401.12345 (2024)

11. Qu, Linhao, Zhang, Chengsheng, Li, Guihui, Zheng, Haiyong, Peng, Chen, He, Wei: Advancing H&E-to-IHC Stain Translation in Breast Cancer: A Multi-Magnification and Attention-Based Approach. In: Proceedings of the IEEE International Conference on Cybernetics and Intelligent Systems (CIS) and IEEE International Conference on Robotics, Automation and Mechatronics (RAM). pp. 441–446 (2024)
12. Dubey, Shikha, Chong, Yosep, Knudsen, Beatrice, Elhabian, Shireen Y: VIMS: virtual immunohistochemistry multiplex staining via text-to-stain diffusion trained on uniplex stains. In: Proceedings of the International Workshop on Machine Learning in Medical Imaging. pp. 143–155 (2024)
13. Yan, Xudong, Yuan, Mingze, Lu, Yao, Zhang, Ying, Chen, Zifan, Bao, Peng, Li, Zehua, Dong, Bin, Yang, Li, Zhang, Li: Versatile Stain Transfer in Histopathology Using a Unified Diffusion Framework. In: bioRxiv. pp. 2024–11 (2024)
14. Liu, Shuting, Zhang, Baochang, Liu, Yiqing, Han, Anjia, Shi, Huijuan, Guan, Tian, He, Yonghong: Unpaired stain transfer using pathology-consistent constrained generative adversarial networks. In: IEEE Transactions on Medical Imaging. pp. 1977–1989 (2021)
15. Xu, Hanwen, Usuyama, Naoto, Bagga, Jaspreet, Zhang, Sheng, Rao, Rajesh, Naumann, Tristan, Wong, Cliff, Gero, Zelalem, González, Javier, Gu, Yu, others: A whole-slide foundation model for digital pathology from real-world data. In: Nature. pp. 1–8 (2024)
16. Song, Jiaming and Meng, Chenlin and Ermon, Stefano: Denoising diffusion implicit models. In: arXiv preprint arXiv:2010.02502. (2020)
17. Nichol, Alex, Dhariwal, Prafulla, Ramesh, Aditya, Shyam, Pranav, Mishkin, Pamela, McGrew, Bob, Sutskever, Ilya, Chen, Mark: Glide: Towards photorealistic image generation and editing with text-guided diffusion models. arXiv preprint arXiv:2112.10741 (2021)
18. Ho, Jonathan, Jain, Ajay, Abbeel, Pieter: Denoising diffusion probabilistic models. In: Advances in Neural Information Processing Systems. pp. 6840–6851 (2020)
19. Rombach, Robin, Blattmann, Andreas, Lorenz, Dominik, Esser, Patrick, Ommer, Björn: High-resolution image synthesis with latent diffusion models. In: Proceedings of the IEEE/CVF Conference on Computer Vision and Pattern Recognition. pp. 10684–10695 (2022)
20. Filiot, Alexandre and Ghermi, Ridouane and Olivier, Antoine and Jacob, Paul and Fidon, Lucas and Camara, Axel and Mac Kain, Alice and Saillard, Charlie and Schiratti, Jean-Baptiste: Scaling self-supervised learning for histopathology with masked image modeling. In: medRxiv. pp. 2023–07 (2023)
21. Brooks, Tim, Holynski, Aleksander, Efros, Alexei A.: Instructpix2pix: Learning to follow image editing instructions. In: Proceedings of the IEEE/CVF Conference on Computer Vision and Pattern Recognition. pp. 18392–18402 (2023)
22. Zhang, Lvmin, Rao, Anyi, Agrawala, Maneesh: Adding conditional control to text-to-image diffusion models. In: Proceedings of the IEEE/CVF International Conference on Computer Vision. pp. 3836–3847 (2023)
23. Tumanyan, Narek, Geyer, Michal, Bagon, Shai, Dekel, Tali: Plug-and-play diffusion features for text-driven image-to-image translation. In: Proceedings of the IEEE/CVF Conference on Computer Vision and Pattern Recognition. pp. 1921–1930 (2023)
24. Hertz, Amir, Aberman, Kfir, Cohen-Or, Daniel: Delta denoising score. In: Proceedings of the IEEE/CVF International Conference on Computer Vision. pp. 2328–2337 (2023)

25. Karras, Tero and Aittala, Miika and Aila, Timo and Laine, Samuli: Elucidating the design space of diffusion-based generative models. In: *Advances in neural information processing systems*. pp. 26565–26577 (2022)
26. Lin, Shanchuan and Liu, Bingchen and Li, Jiashi and Yang, Xiao: Common diffusion noise schedules and sample steps are flawed. In: *Proceedings of the IEEE/CVF winter conference on applications of computer vision*. pp. 5404–5411 (2024)

This figure "etas.png" is available in "png" format from:

<http://arxiv.org/ps/2505.06793v1>